JOURNAL OF AGRICULTURAL AND FOOD CHEMISTRY

Modeling Production of Antifungal Compounds and Their Role in Biocontrol Product Inhibitory Activity

SCOTT W. PRYOR,[†,‡] KARL J. SIEBERT,[§] DONNA M. GIBSON,[||] JAMES M. GOSSETT,[⊥] AND LARRY P. WALKER*[,‡]

Department of Biological and Environmental Engineering, and School of Civil and Environmental Engineering, Cornell University, Ithaca, New York 14853, Food Science and Technology Department, Cornell University, Geneva, New York 14456, and Plant Protection Research Unit, Agricultural Research Service (ARS), United States Department of Agriculture (USDA), Ithaca, New York 14853

Partial least squares (PLS) regression modeling was used to relate the antifungal activity of *Bacillus subtilis* solid-state fermentation extracts to the individual high-performance liquid chromatography (HPLC) peaks from those extracts. A model was developed that predicted bioassay inhibition based on the extract HPLC profile ($R^2 = 0.99$). Concentrations of the members of the antifungal lipopeptide families iturin A and fengycin were found to correlate positively with extract inhibition, but a peak with unidentified chemical composition (designated as peak 48) showed the strongest correlation with extract inhibition. HPLC data were used to construct models for the production of iturin A, fengycin, and peak 48 as a function of the substrate moisture content, incubator temperature, and aeration rate in the solid-state bioreactors. Maximum production of all compounds occurred at the highest moisture content (1.7 g/g dry basis) and lowest incubator temperature (19 °C) tested. Optimal aeration rates for the production of the two known lipopeptides and peak 48 were 0.1 and 1.5 L/min, respectively.

KEYWORDS: Biocontrol; iturin; fengycin; *Bacillus subtilis*; PLS; solid-state fermentation

INTRODUCTION

Bacillus subtilis is a spore-forming bacterium commonly used in commercial and research biocontrol products (BCPs) to control a variety of plant pathogens (*1–4*). Such products may consist of bacterial spores, (fermentation broth containing) biologically active metabolites, or a combination of both. Product efficacy for *B. subtilis* BCPs is thought to be a function of its ability to produce a spectrum of antifungal lipopeptide families, including iturin A, fengycins, plipastatins, and surfactins (*5*). Although the biological activities of many of these individual compounds have been studied (*6–9*), little information is available concerning how they may function in combination. Surfactin has little antifungal activity on its own but has been shown to synergistically enhance the activity of iturin A (*10*). Although *B. subtilis* produces a host of biologically active compounds, it is not clear how each compound affects the overall biological activity in the complex mixture of a BCP. Only limited work has been done on the effect of fermentation conditions on the production of these compounds in submerged fermentation (SMF) or solid-state fermentation (SSF) systems (*11, 12*).

This paper uses data from an optimization of SSF BCP extract activity for further modeling and analysis (*13*). Those optimization results showed that antifungal activity and spore production were both more sensitive to substrate moisture content than to the aeration rate or incubator temperature. The highest levels of each response variable occurred at maximum dry basis (db) moisture contents (1.7 g/g). Maximum antifungal activity was seen in a limited area of the design space (high moisture content, low incubator temperature, and moderate aeration). Spore production, however, was fairly robust with near-maximum levels occurring over a wider range of incubator temperatures and aeration rates. The goals of this paper are (1) to elucidate the relationship between BCP metabolite composition and antifungal activity and (2) to identify fermentation conditions that produce the maximum levels of compounds found to be associated with that activity.

Modeling fungal growth inhibition as a function of high-performance liquid chromatography (HPLC) chromatographic data will allow a more rapid assessment of BCP biological activity without having to use more time-intensive biological assays. Such high-throughput methods for product assessment will speed product development. Individual models developed for the production of specific BCP extract components will help

* To whom correspondence should be addressed: Department of Biological and Environmental Engineering, Cornell University, Ithaca, NY 14853. Telephone: 607-255-2478. Fax: 607-255-4080. E-mail: lpw1@cornell.edu.

[†] Current address: Agricultural and Biosystems Engineering Department, North Dakota State University, Fargo, ND 58105.

[‡] Department of Biological and Environmental Engineering, Cornell University.

[§] Food Science and Technology Department, Cornell University.

[||] United States Department of Agriculture (USDA).

[⊥] School of Civil and Environmental Engineering, Cornell University.

10.1021/jf0719252 CCC: $37.00
Published on Web 10/20/2007

Table 1. Experimental Design and Results from Fermentation Optimization

treatment	aeration rate (L/min)	moisture content (g/g db)	incubator temperature (°C)	iturin A concentration (mg/g)	fengycin (HPLC peak area)	peak 48 (HPLC peak area)
1	0.1	1.00	19	0.893	71.71	3.73
2	0.1	1.00	27	0.593	28.17	2.33
3	0.1	1.70	19	1.274	88.41	5.70
4	0.1	1.70	27	0.569	21.61	3.25
5	1.5	1.00	19	0.778	41.31	2.65
6	1.5	1.00	27	0.569	39.04	3.20
7	1.5	1.70	19	1.172	83.83	9.97
8	1.5	1.70	27	0.751	41.23	5.47
9	0.1	1.35	23	0.752	35.07	4.74
10	1.5	1.35	23	0.904	60.57	7.47
11	0.8	1.00	23	0.822	63.17	4.98
12	0.8	1.70	23	0.848	66.45	6.09
13	0.8	1.35	19	1.006	46.05	6.89
14	0.8	1.35	27	0.652	33.69	4.67
15	0.8	1.35	23	0.808	38.11	6.24
16	0.8	1.35	23	0.804	26.47	5.81
17	0.8	1.35	23	0.855	36.08	6.36
18	0.8	1.35	23	0.835	30.31	5.79
19	0.8	1.35	23	0.780	26.30	5.16

us understand the conditions in which important antifungal compounds are produced either in fermentation reactors or *in situ* after BCP application. The models will also allow for a higher level of product specification based on pathogen susceptibility to BCP components.

MATERIALS AND METHODS

Sample Preparation. *B. subtilis* strain TrigorCor 1448 (*14*) was grown in 0.5 L SSF bioreactors using wheat middlings as a growth substrate (*15*). Growth conditions were optimized for spore production and antifungal activity of product extracts (*13*). Optimization parameters included incubator temperature, aeration, pH buffering, nitrate addition, peptone supplementation, fermentation time, and substrate moisture content. A central composite face-centered experimental design (**Table 1**) was used for response surface modeling of the effects of the incubator temperature, aeration rate, and substrate moisture content on product composition and efficacy. The effects of these parameters on product spore concentrations and extract antifungal activity have already been reported (*13*). Sample extracts from the 19 treatments were prepared and diluted in methanol at a concentration of 80 mg of BCP/mL for HPLC analysis (*13*).

Microbial Inhibition Assays. A 96-well microplate bioassay was used to measure the inhibition of BCP extracts against *Fusarium oxysporum* f. sp. *melonis* (*13*). Extract inhibition was tested by adding 100 μL of potato dextrose broth, 10 μL of BCP extract or solvent control, and 100 μL of a *F. oxysporum* spore suspension (10^4 spores/mL) to each well. BCP extracts were diluted in methanol, and all treatments were measured in triplicate. Plates were read before and after incubating at 25 °C for 48 h using a Synergy HT plate reader (Bio-Tek Instruments, Winooski, VT). Percent inhibition was determined by comparing the absorbance (620 nm) increase of the wells containing the BCP extract with wells containing the control solvent used for extract dilution.

HPLC Analysis. The HPLC method described previously (*15*) was modified to improve peak separation. A System Gold HPLC (Beckman Coulter, Inc., Fullerton, CA) was used for all separations. Samples were injected onto a Varian Polaris (Palo Alto, CA) 5 μm C18 column (4.6 × 250 mm) and eluted at a flow rate of 1 mL/min. Gradient conditions were as follows: [acetonitrile (A) and water (B), each with 0.1% trifluoroacetic acid] 0–1 min, 45% A; 1–31 min, 45–65% A; 31–41 min, 65–88% A; 41–51 min, 88% A; and 51–59 min, 45% A. The elution profile was monitored with a photodiode-array (PDA) detector over the UV absorbance range of 194–350 nm. Injections of 20 μL were made with extract concentrations of 80 mg of BCP/mL in methanol.

Several larger peaks common to all extracts were identified from the HPLC data and used as chromatogram reference points. All peaks eluting between these references were time-scaled to account for minor variations in elution times between samples. From the data profiles, 61 peaks found to be present in all or most of the samples were used for modeling.

A representative BCP extract sample was further fractionated for peak identification by mass spectrometry. A 20 μL volume of a sample extract diluted to 50 mg of extract/mL (4.27 g of BCP/mL) was separated using the described HPLC system and a Foxy 200 fraction collector (Isco, Lincoln, NE). Fractions were collected in 12 s increments and pooled to analyze individual peak components. These pooled HPLC fractions in the original mobile phase [mixtures of acetonitrile (0.1% TFA)/H_2O (0.1% TFA)] were infused into a Micromass ZMD-4000 (Waters Corporation, Milford, MA) spectrometer at 5 μL/min with a syringe pump (Harvard Apparatus, Holliston, MA). Low-resolution electrospray ionization mass spectrometry (ESI–MS) spectra were acquired in the positive-ion mode using a capillary voltage of 4 kV and sample cone voltages of 40 and 80 V.

Modeling. *PLS Inhibition Modeling.* Partial least squares (PLS) regression modeling was done using the Simca-S software (Umetrics, Umea, Sweden) to determine relationships between individual chromatographic peaks and overall extract inhibition. PLS regression is a widely used analysis tool in the chemometrics field (*16*). In addition to modeling the date data, PLS produces a variable importance to the projection (VIP) parameter that shows the relative value of each predictor variable to the PLS model (*16*). The final PLS model relates each individual HPLC peak area to extract inhibition in the form of eq 1.

$$y = \beta_0 + \sum_{i=1}^{n} \beta_i A_i \quad (1)$$

where y is the extract inhibition at 20 mg of BCP/mL in the microplate bioassay, β_0 is the model constant term, i is the peak number (in order of decreasing VIP), n is the total number of peaks (61) in the model, β_i is the linear coefficient associated with peak i, and A_i is the area under the curve of HPLC peak i.

Aggregate Component Inhibition Modeling. Groups of peaks identified through PLS modeling were combined for additional inhibition modeling to better understand the role of compound families on extract inhibition. Peaks were pooled in several combinations according to their chemical composition (iturin A, fengycin, or other components) as determined from mass spectrometry (MS) analysis. HPLC peak areas for groups of peaks were summed and related to extract inhibition with a linear least-squares regression. Regression modeling was done using a MATLAB (The MathWorks, Inc., Natick, MA) program to estimate model coefficients for the following equation:

$$y = \alpha_0 + \sum_{j} \alpha_j z_j \quad (2)$$

where y is the extract inhibition at 20 mg of BCP/mL in the microplate bioassay, α_0 is the model constant term, α_j is the linear coefficient associated with peaks in group j, z_j is the area under the curve of HPLC peaks for group j, and j is the peak grouping (i.e., iturin A, fengycin, etc.).

Extract Component Modeling. HPLC peak data were used to generate response surfaces for iturin A, and fengycin, and peak 48 production as a function of the incubator temperature, aeration rate, and substrate moisture content. Data for each lipopeptide were transformed by a square-root function prior to modeling to reduce the lack of fit statistic. A MATLAB program was written to estimate model parameters for the following equation:

$$y = b_0 + b_1x_1 + b_2x_2 + b_3x_3 + b_4x_1^2 + b_5x_2^2 + b_6x_3^2 + b_7x_1x_2 + b_8x_1x_3 + b_9x_2x_3 \quad (3)$$

where y is the response variable (measure of lipopeptide concentration), b_{0-9} are the model parameters, x_1 is the aeration level (in L/min), x_2 is the substrate initial dry basis moisture content (in g/g), and x_3 is the incubator temperature (in °C).

The MATLAB program was also used to determine theoretical stationary points and local maxima within the design space, create analysis of variance (ANOVA) tables for models, and plot response surface model results. Models were developed using a linear least-squares method described previously (*13*).

Model coefficients were tested for significance using SPSS software (SPSS, Inc., Chicago, IL); parameters whose coefficients had a p value greater than 0.05 were sequentially removed to determine the effect of the parameter on the model R^2 and R^2_{adj} values. Parameters were permanently removed from the model when it was seen that their inclusion had a negative impact on R^2_{adj} values.

RESULTS

PLS Regression. HPLC chromatograms from each of the 19 samples were analyzed concurrently, and 61 common individual peaks were identified for PLS regression analysis. The 61 chromatographic peaks were used to develop a model predicting microplate bioassay inhibition levels against *F. oxysporum* at 20 mg of BCP/mL. This concentration was chosen because the extract inhibition data points at this concentration showed the greatest spread and facilitated sample differentiation (*13*). During analysis, 16 peaks with VIP coefficients less than 0.55 were identified as not contributing significantly to the model and were removed, leaving 45 peaks. Model coefficients for the constant term and each peak, in order of VIP, are shown in **Table 2**. The resultant model had R^2 and Q^2 (cross-validated R^2) values of 0.988 and 0.811, respectively. The Q^2 value is a conservative estimate of the predictive capability of the model when using new data. Observed versus predicted values are plotted in **Figure 1**. A normal probability plot of residuals showed no deviation from normality (data not shown).

The nine most influential (shown in **Figure 2**), as determined by VIP value (shown in **Figure 2**), were chosen for further analysis by MS. Most of these peaks were positively related to inhibition, as shown by the model coefficients in **Table 2**.

Results of MS analysis for those peaks are shown in **Table 3**. Peaks 4, 5, and 8 were all identified as belonging to the iturin A family and were positively correlated with extract inhibition. PDA spectra for these peaks also matched with an iturin A standard (data not shown). Peaks 31, 38, and 43 all contained mass ions associated with fengycin homologues. Peak 38 was negatively related to extract inhibition, while peaks 31 and 43 showed a positive relationship with inhibition.

Additional peaks were also examined by MS. Two additional peaks were found to have the same molecular weight as iturin A homologues, while 14 more peaks eluting between 26 and 41 min contained compounds with molecular weights equivalent to known fengycin components. Although peaks 48, 51, and 56 all had high VIP values, mass spectra from these peaks did not match with masses of surfactins or other antibiotics known to be produced by *B. subtilis*.

Aggregate Component Modeling. It was noted through PLS modeling that component peaks of iturin A and fengycin together with peaks with unidentified chemical composition (i.e., peaks 48 and 51) were associated most strongly with the antifungal activity of BCP extracts. In an attempt to simplify the model, HPLC peak area data were pooled according to individual peak chemical identification. PLS modeling showed that individual peaks identified as either iturin A or fengycin homologues could have either a positive or negative correlation with extract inhibition as reflected by model coefficients in **Table 2**. Iturin A and fengycin groups were divided into peaks with positive and negative PLS model coefficients. The combined data were then used for linear least-squares regression modeling to examine the relationship between groups of individual peaks and extract inhibition.

Models were developed including several different combinations of peak groupings. Peak 51 was included in modeling

Table 2. PLS Regression Modeling of HPLC Peak Area and Microplate Inhibition Data

coefficient[a]	VIP	coefficient value
β_0		0.109
β_{48}	1.73	0.011
β_{51}	1.65	0.040
β_4	1.49	0.028
β_{56}	1.36	−0.223
β_{38}	1.36	−0.027
β_5	1.31	0.006
β_8	1.30	0.007
β_{43}	1.30	0.146
β_{31}	1.27	0.010
β_{35}	1.15	−0.021
β_{61}	1.11	0.088
β_{46}	1.05	−0.216
β_{33}	1.04	0.032
β_{23}	1.04	0.008
β_{20}	0.99	0.010
β_2	0.97	−0.032
β_9	0.94	0.007
β_{27}	0.94	−0.010
β_{15}	0.92	0.102
β_{18}	0.91	0.027
β_{40}	0.91	0.060
β_{36}	0.91	0.029
β_{39}	0.90	0.043
β_1	0.89	−0.001
β_{50}	0.88	−0.070
β_{49}	0.88	−0.057
β_{11}	0.87	−0.026
β_{32}	0.87	0.063
β_{42}	0.86	0.378
β_3	0.85	−0.059
β_{21}	0.83	−0.017
β_{16}	0.81	0.007
β_{24}	0.81	0.008
β_{45}	0.79	0.012
β_6	0.79	0.003
β_{25}	0.74	0.003
β_{52}	0.73	0.012
β_{13}	0.72	−0.004
β_{12}	0.71	−0.0338
β_{26}	0.69	−0.0023
β_{29}	0.63	−0.0002
β_{22}	0.61	−0.0006
β_{47}	0.60	−0.1341
β_{59}	0.60	−0.0067
β_{41}	0.58	0.0590

[a] The parameter subscript denotes the HPLC peak number.

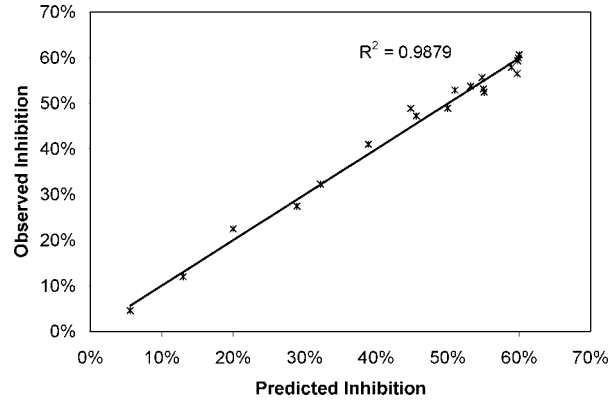

Figure 1. Comparison of the observed fungal inhibition and that predicted by the PLS model based on HPLC peak areas.

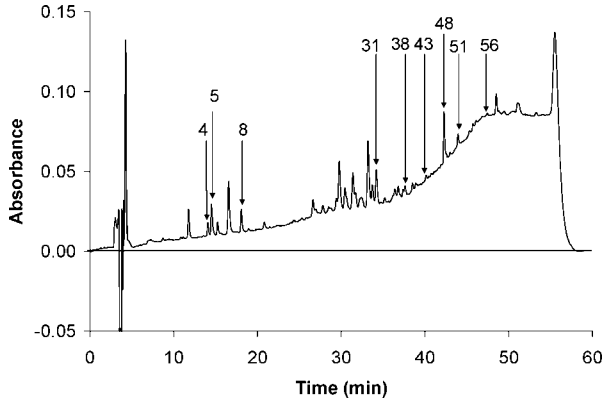

Figure 2. HPLC peaks selected for MS analysis.

Table 3. Summary of the Results of MS Analysis of Selected HPLC Peaks in Order of VIP

peak number	mass ion (*m*/*z*)	assignment
48		unknown
51		unknown
4	1057.3 $(M + H)^+$, 1079.4 $(M + Na)^+$	iturin A
56		unknown
	724.4 $(M + 2H)^{+2}$	unknown
38	731.5 $(M + 2H)^{+2}$	unknown
	753.4 $(M + 2H)^{+2}$	fengycin B (C17)
5	1057.3 $(M + H)^+$, 1079.3 $(M + Na)^+$	iturin A
8	1071.5 $(M + H)^+$, 1093.6 $(M + Na)^+$	iturin A
43	760.6 $(M + 2H)^{+2}$	fengycin B (C18)
	739.5 $(M + 2H)^{+2}$	fengycin A (C17), B (C15)
31	746.5 $(M + 2H)^{+2}$, 757.5 $(M + H + Na)^{+2}$	fengycin A (C18), B (C16)

either as an individual component or in combination with peak 48, but its inclusion did not yield significant model improvements. Similarly, inclusion of fengycin peaks negatively correlated with inhibition did not improve the model. Model adequacy was based on model fit (R^2 and R^2_{adj} values) and simplicity in terms of the total number of parameters. The best model based on these criteria was

$$y = 5.07z_1 - 7.73z_2 + 1.171z_3 + 2.08z_4 \quad (4)$$

where z_1 is the sum of HPLC peak areas for all iturin A peaks with positive PLS model coefficients, z_2 is the sum of HPLC peak areas for all iturin A peaks with negative PLS model coefficients, z_3 is the sum of HPLC peak areas for all fengycin peaks with positive PLS model coefficients, and z_4 is the HPLC peak area for peak 48.

The R^2 and R^2_{adj} values for this model were 0.825 and 0.790, respectively. This final model fits the data well and is in agreement with earlier work presented here. According to the model, iturin A, fengycin, and peak 48 all contribute positively to extract inhibition as shown in the PLS model. The addition of the iturin A peak with a negative PLS coefficient confirmed the negative effect of the peak and yielded significant model improvements.

Iturin A Quantification and Modeling. Five major peaks were identified as belonging to the iturin A family through chromatographic comparison with an iturin A standard and subsequent molecular-weight confirmation by MS. The HPLC areas for these peaks were summed, and an eight-point iturin A standard curve ($R^2 = 0.9996$, data not shown) was used to convert HPLC peak areas into units of mg of iturin A/g of dry BCP. All iturin A peaks were assumed to have the same response factor for standard curve development.

Table 4. ANOVA Table for the Model of Iturin A Production[a]

source of variation	sum of squares	degrees of freedom	mean square	F_0	*p* value
regression	0.560	6	0.093	29.55	0.0002
residual	0.038	12	0.0032		
lack of fit	0.035	8	0.0043	5.26	0.063
pure error	0.0033	4	0.000 83		
total	0.59	18	0.033		

[a] The R^2 value for the model is 0.937, and the R^2_{adj} value is 0.905.

Iturin A concentrations (**Table 1**) were used to create a response surface model (in the form of eq 3) of the square root of iturin production as a function of aeration, moisture content, and incubator temperature. Quadratic terms associated with each of the main factors were found to be negligible and were removed from the model before re-evaluating the parameters. The resulting equation was squared to yield the final model of iturin A production (mg/g dry BCP)

$$y = (0.31 - 0.52x_1 + 1.45x_2 + 0.01x_3 + 0.11x_1x_2 + 0.02x_1x_3 - 0.06x_2x_3)^2 \quad (5)$$

The ANOVA table for the model (**Table 4**) shows that the significance of the regression is very high ($p = 0.0002$). The lack of a fit test, although not significant at the 95% confidence level, is higher than would be desirable ($p = 0.0630$). This is primarily due to the fact that chromatographic peaks for iturin A and other components in replicate treatments were very similar in peak areas, resulting in a low pure error component of the residual mean square. The high level of significance of the regression together with the high R^2 and R^2_{adj} values (0.937 and 0.905, respectively) indicate an acceptable model. Further, a plot of residuals versus predicted values from the model revealed no model inadequacy.

Figure 3 shows contour plots of the model at dry basis moisture contents of 1, 1.35, and 1.7 g/g. These results show that iturin A production is highly sensitive to the incubator temperature. Initial substrate moisture content also has a strong effect on iturin A production but primarily when the incubator temperature is low. The highest concentrations of iturin A (approximately 1.4 mg/g dry BCP) were produced at the lowest incubator temperature (19 °C) and highest dry basis moisture content (1.7 g/g) in the study. Aeration rates did not have a significant impact in this area of the design space, but the model generally shows that reactors tend to produce more iturin A operating at lower aeration rates.

Fengycin Modeling. A similar analysis was completed for peaks associated with fengycins. At least 18 peaks were identified as containing a fengycin component. HPLC peak areas were summed for all of these peaks, and the total area (**Table 1**) was used for estimating model parameters. The quadratic terms associated with the aeration rate and incubator temperature and the aeration–moisture content interaction term were found not to be significant at the 95% confidence level. These terms were removed from the model before re-evaluating the parameters. The resulting equation was squared to yield the final model of total fengycin production (sum of the HPLC peak area/1.6 mg of dry BCP) as shown in eq 6

$$y = (21.6 - 4.81x_1 - 16.7x_2 + 0.026x_3 + 9.71x_2^2 + 0.223x_1x_3 - 0.370x_2x_3)^2 \quad (6)$$

The ANOVA table for the model is shown in **Table 5**. Similar to the iturin A model, the ANOVA table shows that the probable

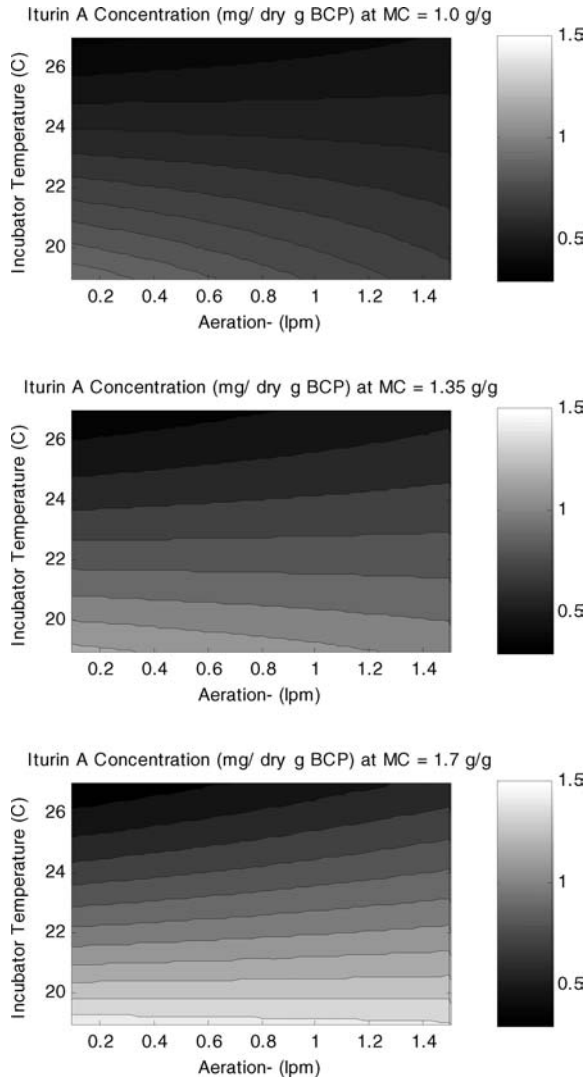

Figure 3. Results of the response surface modeling of iturin A yield as a function of aeration, incubator temperature, and moisture content (MC).

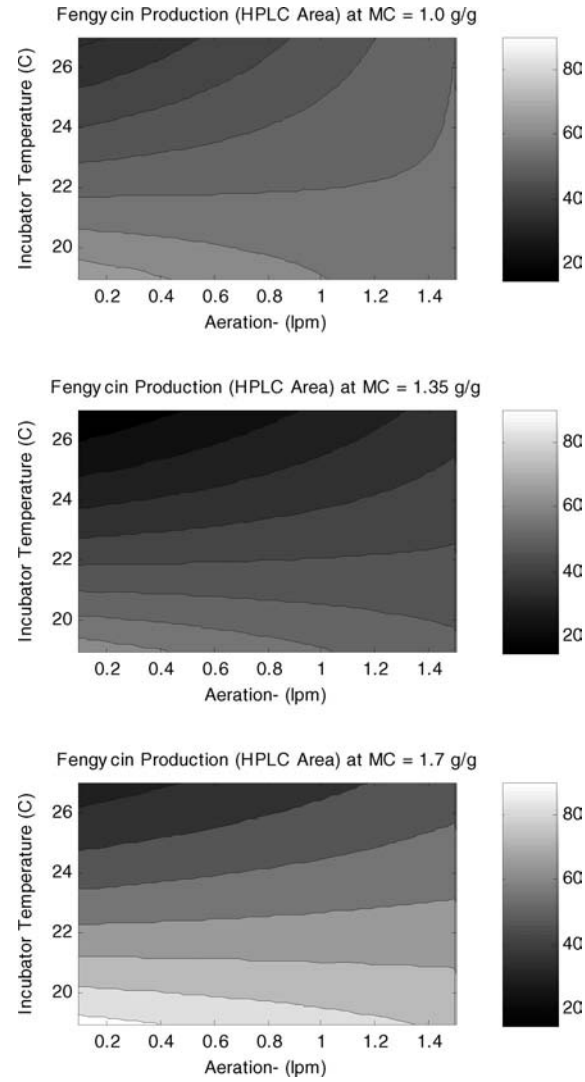

Figure 4. Results of the response surface modeling of fengycin yield (HPLC peak area) as a function of aeration, incubator temperature, and MC.

Table 5. ANOVA Table for the Model of Fengycin Production[a]

source of variation	sum of squares	degrees of freedom	mean square	F_0	p value
regression	27.6	6	4.60	6.38	0.003
residual	8.66	12	0.72		
lack of fit	7.72	8	0.965	4.14	0.093
pure error	0.93	4	0.233		
total	36.25	18	2.014		

[a] The R^2 value for the model is 0.761, and the R^2_{adj} value is 0.642.

significance of the regression is very high, while the lack of the fit test, although not significant at the 95% confidence level, had a lower p value than would be desired. The fengycin model appears acceptable, with R^2 and R^2_{adj} values of 0.761 and 0.642, respectively. It does not, however, fit as well as the iturin A model. Again, a plot of residuals versus predicted values and a normal probability plot of residuals (results not shown) revealed no model inadequacy.

Figure 4 shows the contour plot of the fengycin model at dry basis moisture contents of 1, 1.35, and 1.7 g/g. These results show that, at high moisture contents, the pattern of fengycin production is very similar to that of iturin A production. High moisture content and low incubator temperature are the most important parameters in fengycin production. Production is fairly robust across aeration rates, but the model predicts somewhat higher concentrations at low aeration rates.

Peak 48 Modeling. Peak 48 was chosen for further analysis and modeling because it was shown to be the most important parameter in the inhibition model according to VIP values. Peak 51 was also shown to have a high model importance and was positively correlated ($R^2 = 0.705$) with peak 48 levels (data not shown). HPLC peak area data for peak 48 are included in **Table 1**. The quadratic term associated with the aeration rate and the aeration–incubator temperature interaction term were found not to be significant at the 95% confidence level. These terms were removed from the model before re-evaluating the parameters. The final model for peak 48 production (HPLC area/1.6 mg of dry BCP) is as shown in eq 7

$$y = -39.2 - 3.3x_1 + 31.9x_2 + 2.2x_3 - 6.76{x_2}^2 + -0.04{x_3}^2 + 3.4x_1x_2 - 0.54x_2x_3 \quad (7)$$

The ANOVA table for the model is shown in **Table 6**. The ANOVA table again shows a high significance of the regression ($p = 0.0001$) and no significance for the lack of fit ($p = 0.147$). The R^2 and R^2_{adj} values are 0.905 and 0.844, respectively.

Table 6. ANOVA Table for the Model of Peak 48 Production[a]

source of variation	sum of squares	degrees of freedom	mean square	F_0	p value
regression	54.4	7	7.77	14.95	0.0001
residual	5.72	11	0.52		
lack of fit	4.82	7	0.69	3.08	0.147
pure error	0.90	4	0.22		
total	60.1	18	3.34		

[a] The R^2 value for the model is 0.905, and the R^2_{adj} value is 0.844.

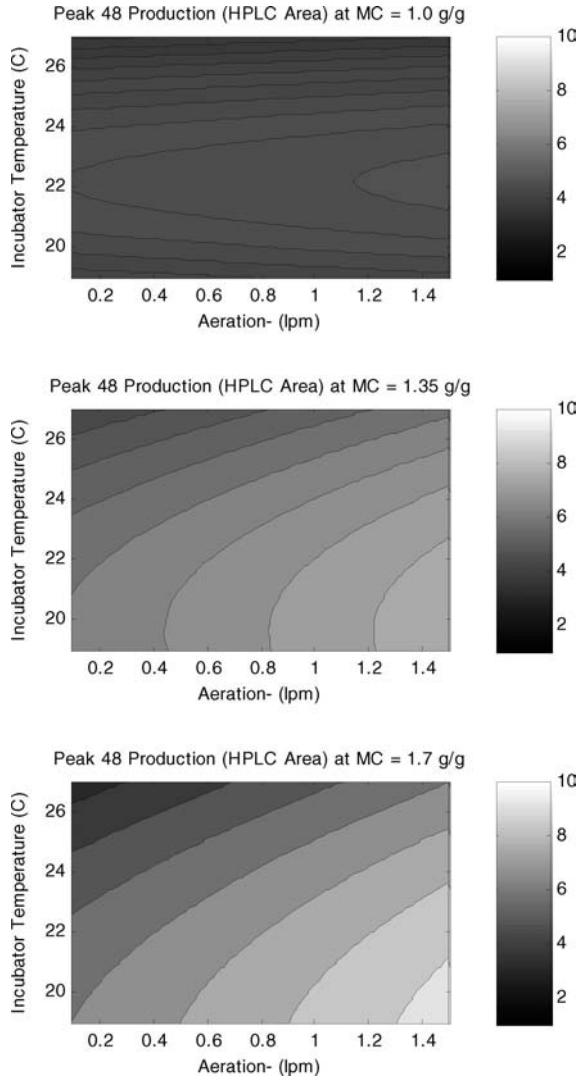

Figure 5. Results of the response surface modeling of peak 48 yield (HPLC peak area) as a function of aeration, incubator temperature, and MC.

Figure 5 shows the contour plots of the model at dry basis moisture contents of 1, 1.35, and 1.7 g/g. These results show that, at constant moisture content, the pattern of peak 48 production is significantly different to that of iturin A or fengycin production with respect to the importance of aeration. The moisture content, incubator temperature, and aeration rate were all shown to have significant effects on production levels. Maximum values occurred at the highest moisture content (1.7 g/g), lowest incubator temperature (19 °C), and highest aeration rates (1.5 L/min) tested.

DISCUSSION

The PLS regression model developed draws correlative relationships between the BCP extract HPLC peak area data and the antifungal activity of those extracts. The development of a PLS model to predict bioassay inhibition based on the HPLC chromatographic profile is useful for several reasons. HPLC analyses of BCP extracts are faster and more precise than bioassays, and such a model allows for a higher throughput method for fermentation screening. Peaks with high VIP values can be examined more thoroughly to determine the chemical structure and antifungal activity. Those peaks with strongly positive or strongly negative correlation coefficients can be evaluated as individual compounds rather than as part of composite groups.

The predictive activity model also allows for the estimation of bioassay EC_{50} (effective concentration for 50% control) values as an alternative means of quantifying activity between extracts. Extracts with similar inhibitory properties at a given concentration may have dissimilar dose–response curves, making EC_{50} a more accurate quantification of the overall activity.

Aggregate modeling confirmed the importance of iturin A, fengycin, and peak 48 to BCP extract inhibition, as suggested in PLS modeling results. These lumped parameter models provide a clearer link between BCP extract chemical composition and the inhibitory quality of that extract. Because the relative importance of each model component (positively and negatively correlated iturin A components, positively correlated fengycin components, and peak 48) is different, the overall extract inhibition depends upon the extract composition. These model results show that peak 48 accounts for approximately 25% of the total activity within this data set, while iturin A and fengycin each account for 38%.

Of the five major peaks identified as iturin A, all but one were positively correlated with extract inhibition. One iturin A component (peak 1) was negatively correlated with inhibition and had a molecular weight of 1042 Da, the lowest of all iturin A homologues found. Its negative relationship with extract inhibition was confirmed by further aggregate modeling. Molecular-weight differences between iturin A species are indicative of the length of the carbon tail attached to the peptide ring. Lipopeptides with longer carbon tails have been shown to have stronger antifungal activity than those with shorter tails (*17*). These results indicate that it is important to consider the iturin A constituent fraction composition, as well as the total mass, during BCP production.

Of the 18 fengycin components found, 10 were found to correlate positively with inhibition, while 4 showed a negative correlation and 3 were negligible and removed from the model. No relationship was apparent between inhibition and component molecular weight as was seen for iturin A.

Although the incubator temperature is shown to be an important factor in the solid-state production of iturin A, the relationship between the maximum reactor temperature (model not shown) and iturin A production is not well-defined. The reactor temperature may be limited with low incubator temperatures, low moisture contents, or high aeration rates. Although each of these fermentation conditions can be adjusted to control maximum reactor temperatures, only by decreasing incubator temperatures was iturin A production substantially increased. Lowering the moisture content has an overall negative effect on total iturin A production. In the case of low moisture contents, iturin A yield gains from the resultant reactor temperature control are lost because of the lower cell mass found with these conditions (*13*). Likewise, increasing the reactor aeration rate generally decreases the final product spore counts.

High moisture contents improve iturin A yields partially because of increased cell mass. High moisture contents increase

biofilm volume per dry gram of substrate, effectively increasing the usable space within the bioreactor. The interaction with temperature, however, is evident because high spore counts ($>2.5 \times 10^{10}$ spores/dry g) can be seen at incubator temperatures of 27 °C and moisture contents as low as 1.35 g/g (*13*).

Interestingly, SSF models of iturin A and fengycin production were very similar to one another but do not match with models of oxygen use (data not shown) or spore production (*13*). There are some similarities between models of inhibition and lipopeptide production because maximum levels of each are seen at high substrate moisture contents and low incubator temperatures. Aeration, however, has a strong positive effect on inhibition and a lesser negative effect on lipopeptide production. Aeration rates for producing maximum inhibition are highest at an aeration rate of 1.0 L/min, with levels dropping steadily with aeration rates less than 0.7 L/min. It is expected that both fengycin and iturin A play a role in extract inhibition because their antifungal properties have been documented (*18*, *19*). In addition, extract fractions containing these compounds were found to contain the majority of the activity of the nonseparated extract (*15*). The contrast in models for extract inhibition and lipopeptide production, however, indicate that there may be additional compounds produced at higher aeration rates that play a significant role in the overall activity.

The model developed for peak 48 was significantly different than those for either iturin A or fengycin. This suggests that fermentation conditions could be controlled to alter the metabolite profile. BCPs from *B. subtilis* or other organisms could thus be tailored to specific pathogens based on susceptibility to specific compounds.

Unlike models for iturin A or fengycin production, aeration has a strong positive effect on peak 48 production. The resultant model for peak 48 production matches much more closely with the overall inhibition model (*13*). Because the MS mass ions of this peak did not match with any known antibiotics produced by *B. subtilis*, it may represent a new chemistry produced by this strain. Further work is in progress to characterize the antifungal activity and chemical structure of this peak.

In conclusion, PLS and subsequent aggregate component modeling showed the importance of iturin A, fengycin, and the unidentified peak 48 in the inhibition of *F. oxysporum* in microplate bioassays. Both models allow for the prediction of antifungal activity based on the HPLC profile of the BCP extract. Such models will allow for higher throughput screening of fermentation conditions to produce higher concentrations of lipopeptides or other antifungal metabolites. Further response surface modeling of iturin A and fengycin showed that these compounds have very similar production profiles and are likely regulated through similar pathways. Peak 48, however, was shown to have a different production profile, and the correlation between it and the overall antifungal activity suggests further exploration of this peak chemistry.

ACKNOWLEDGMENT

We thank Drs. Gary Bergstrom and Tom Zitter in the Department of Plant Pathology at Cornell University for providing cultures of *B. subtilis* and *F. oxysporum*, respectively. We also thank Dr. Stuart Krasnoff (U.S. department of Agriculture ARS Plant Protection Research Unit, Ithaca, NY) for his assistance with MS analyses.

LITERATURE CITED

(1) Brannen, P. M.; Kenney, D. S. Kodiak—A successful biological-control product for suppression of soil-borne plant pathogens of cotton. *J. Ind. Microbiol. Biotechnol.* **1997**, *19* (3), 169–171.

(2) Broggini, G. A. L.; Duffy, B.; Holliger, E.; Scharer, H. J.; Gessler, C.; Patocchi, A. Detection of the fire blight biocontrol agent *Bacillus subtilis* BD170 (Biopro) in a Swiss apple orchard. *Eur. J. Plant Pathol.* **2005**, *111* (2), 93–100.

(3) Cavaglieri, L.; Orlando, J.; Rodriguez, M. I.; Chulze, S.; Etcheverry, M. Biocontrol of *Bacillus subtilis* against *Fusarium verticillioides* in vitro and at the maize root level. *Res. Microbiol.* **2005**, *156* (5–6), 748–754.

(4) Szczech, M.; Shoda, M. The effect of mode of application of *Bacillus subtilis* RB14-C on its efficacy as a biocontrol agent against *Rhizoctonia solani*. *J. Phytopathol.* **2006**, *154* (6), 370–377.

(5) Mannanov, R. N.; Sattarova, R. K. Antibiotics produced by *Bacillus* bacteria. *Chem. Nat. Compd.* **2001**, *37* (2), 117–123.

(6) Moyne, A. L.; Shelby, R.; Cleveland, T. E.; Tuzun, S. Bacillomycin D: An iturin with antifungal activity against *Aspergillus flavus*. *J. Appl. Microbiol.* **2001**, *90* (4), 622–629.

(7) Besson, F.; Peypoux, F.; Michel, G.; Delcambe, L. Antifungal activity upon *Saccharomyces cerevisiae* of iturin-A, mycosubtilin, bacillomycin-L and of their derivatives—Inhibition of this antifungal activity by lipid antagonists. *J. Antibiot.* **1979**, *32* (8), 828–823.

(8) Yamada, S.; Takayama, Y.; Yamanaka, M.; Ko, K.; Yamaguchi, I. Biological activity of antifungal substances produced by *Bacillus subtilis*. *J. Pestic. Sci.* **1990**, *15* (1), 95–96.

(9) Vanittanakom, N.; Loeffler, W.; Koch, U.; Jung, G. Fengycin—A novel antifungal lipopeptide antibiotic produced by *Bacillus subtilis* F-29-3. *J. Antibiot.* **1986**, *39* (7), 888–901.

(10) Thimon, L.; Peypoux, F.; Magetdana, R.; Roux, B.; Michel, G. Interactions of bioactive lipopeptides, iturin-A and surfactin from *Bacillus subtilis*. *Biotechnol. Appl. Biochem.* **1992**, *16* (2), 144–151.

(11) Akpa, E.; Jacques, P.; Wathelet, B.; Paquot, M.; Fuchs, R.; Budzikiewicz, H.; Thonart, P. Influence of culture conditions on lipopeptide production by *Bacillus subtilis*. *Appl. Biochem. Biotechnol.* **2001**, *91*, 551–561.

(12) Jacques, P.; Hbid, C.; Destain, J.; Razafindralambo, H.; Paquot, M.; De Pauw, E.; Thonart, P. Optimization of biosurfactant lipopeptide production from *Bacillus subtilis* S499 by Plackett–Burman design. *Appl. Biochem. Biotechnol.* **1999**, *77–79*, 223–233.

(13) Pryor, S. W.; Gibson, D. M.; Hay, A. G.; Gossett, J. M.; Walker, L. P. Optimization of spore and antifungal lipopeptide production during the solid state fermentation of *Bacillus subtilis*. *Appl. Biochem. Biotechnol., Part A* **2007**, in press.

(14) Bergstrom, G. C.; da Luz, W. C. Biocontrol for plants with *Bacillus subtilis*, *Pseudomonas putida*, and *Sporobolomyces roseus*. U.S. Patent 6,896,883 B2, 2005.

(15) Pryor, S. W.; Gibson, D. M.; Krasnoff, S. B.; Walker, L. P. Identification of antifungal compounds in a biological control product using a microplate inhibition bioassay. *Trans. ASAE* **2006**, *49* (5), 1643–1649.

(16) Wold, S.; Sjostrom, M.; Eriksson, L. PLS-regression: A basic tool of chemometrics. *Chemom. Intell. Lab. Syst.* **2001**, *58* (2), 109–130.

(17) Phae, C. G.; Shoda, M. Expression of the suppressive effect of *Bacillus subtilis* on phytopathogens in inoculated composts. *J. Ferment. Bioeng.* **1990**, *70* (6), 409–414.

(18) Viswanathan, P.; Surlikar, N. R. Production of α-amylase with *Aspergillus flavus* on *Amaranthus* grains by solid-state fermentation. *J. Basic Microbiol.* **2001**, *41* (1), 57–64.

(19) Magetdana, R.; Peypoux, F. Iturins, a special class of pore-forming lipopeptides—Biological and physicochemical properties. *Toxicology* **1994**, *87* (1–3), 151–174.

Received for review June 28, 2007. Revised manuscript received September 20, 2007. Accepted September 21, 2007. This research was supported in part through a U.S. Department of Agriculture MGET (Multi-Disciplinary Graduate Education Traineeship) program grant.

JF0719252